RAPID COMMUNICATIONS

PHYSICAL REVIEW B VOLUME 32, NUMBER 2 15 JULY 1985

Ellipsoidal shell structure in free-electron metal clusters

Keith Clemenger
Physics Department, University of California, Berkeley, California 94720
(Received 13 March 1985)

The possibility of ellipsoidal distortions in free-electron metal clusters, analogous to the shape variations among atomic nuclei, is investigated with the use of a modified Nilsson Hamiltonian. In most cases, the predicted equilibrium shape is ellipsoidal rather than spherical, so that the spherical shells are divided into ellipsoidal subshells. A strong correlation is observed between the energy-level sequence of these subshells and the sequence of peaks in alkali-metal cluster mass spectra, indicating that metal clusters generally assume approximately ellipsoidal shapes.

Spherical electronic shell structure has been observed[1,2] in the mass spectra of sodium and potassium clusters produced by supersonic expansion, in agreement with several theoretical analyses.[3,4] A representative mass spectrum of sodium clusters is shown in Fig. 1(a). Major spherical-shell edges have been identified for clusters containing $N=2$, 8, 20, 40, 58, and 92 atoms; and the excellent correspondence of theory and experiment for these numbers indicates a clearly developed spherical-shell structure. The smaller peaks, however, e.g., $N=12$, 14, 26, 30, 34, 36, 38, 50, and 54, cannot all be understood in the framework of strictly spherical theories, which inevitably contain the $2l+1$ orbital degeneracy associated with spherical symmetry. These minor features are nonetheless reproducible under a wide range of experimental conditions for sodium,[1] and several of them are also seen in potassium-cluster mass spectra.[2] In this paper an axially symmetric independent-electron model is employed in an attempt to include both major and minor features in a consistent way.

A successful shell theory for axially symmetric distortions was developed for nuclei by Nilsson.[5,6] Applying his discussion to clusters, we neglect spin-orbit coupling and describe the states of the valence electrons of the cluster by the effective single-particle Hamiltonian

$$H=\frac{\mathbf{p}^2}{2m}+\tfrac{1}{2}m\omega_0^2(\Omega_\perp^2\rho^2+\Omega_z^2 z^2)-U\hbar\omega_0(l^2-\langle l^2\rangle_n)\ , \tag{1}$$

$$\rho^2=x^2+y^2\ , \tag{1a}$$

$$\langle l^2\rangle_n=\tfrac{1}{2}n(n+3)\ , \tag{1b}$$

where the ellipsoidal scaling factors may be expressed in terms of a distortion parameter δ by the equations

$$\Omega_\perp=\left(\frac{2+\delta}{2-\delta}\right)^{1/3}\ , \tag{2a}$$

$$\Omega_z=\left(\frac{2+\delta}{2-\delta}\right)^{-2/3}\ , \tag{2b}$$

assuming the constant-volume constraint $\Omega_\perp^2\Omega_z=1$. To first order, the absolute value of δ is the difference between the major and minor axes of any equipotential surface of the cluster, divided by the mean radius. The ellipsoidal harmonic-oscillator potential is perturbed with an l^2 term to split the dynamical symmetry degeneracies in the spherical oscillator case between different angular momentum states with the same total oscillator quantum number n.[7] If the parameter U is taken to be positive, this effectively flattens the bottom of the potential well and gives it sharper edges.[8] An initial estimate of appropriate U values may be made by matching ratios of energy-level splittings for various values of U with the corresponding ratios from self-consistent jellium calculations;[9] this gives values in the range $0.04<U<0.08$ for most sodium clusters of interest.

The energy scale of the potential well is determined by ω_0, the characteristic frequency of oscillation in the spherical harmonic-oscillator limit ($\delta=0, U=0$). The magnitude of

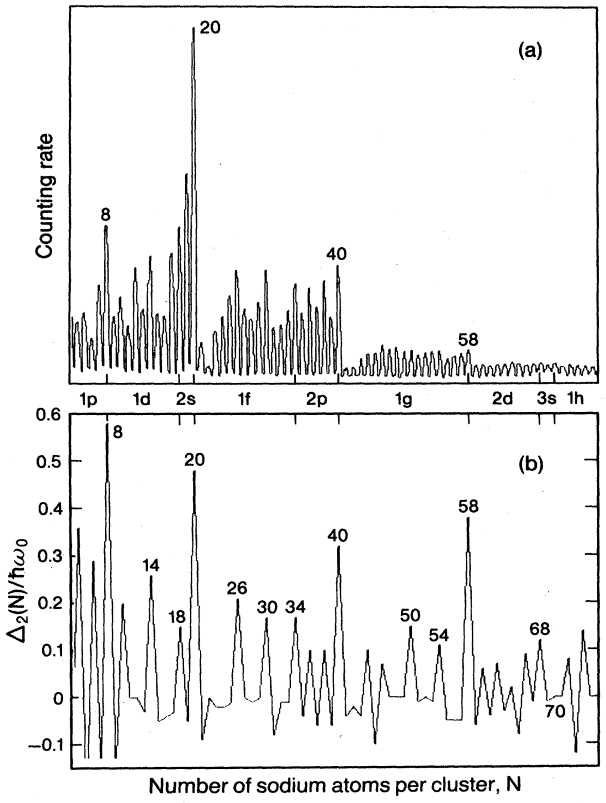

FIG. 1 (a) Experimental mass spectrum of sodium clusters from Ref. 1. The number of atoms per cluster N (which is also the number of valence electrons) is shown for selected clusters. (b) Second difference of the sum of single-particle energies as a function of N, with $U=0.04$. See text for discussion.

ω_0 decreases with increasing N, roughly as $N^{-1/3}$; the results of this paper will be presented in dimensionless form, in units of ω_0, so that no assumption concerning the explicit functional dependence on N need be made. We will only assume that the variations in ω_0 between clusters adjacent in N are negligible.

The solution for the energy eigenvalues is displayed as a function of δ in Fig. 2. For small δ, the spherical representation $|\nu l\rangle$ is most appropriate for describing the eigenstates of the Hamiltonian, with the slight asphericity considered as a perturbation which splits the otherwise degenerate levels within a given l orbital. We adopt the nuclear physics convention that the radial quantum number ν is taken to be 1 for the lowest energy state of given l, $\nu=2$ for the next state with the same l, etc. For large δ the cylindrical representation $|nn_z\Lambda\rangle$ more closely matches the eigenstates, in which n is the total number of oscillator quanta, n_z the number of oscillator quanta in the axial direction, and Λ the projection of the orbital angular momentum along the axis of symmetry.[10] Levels differing only in the sign of Λ are degenerate with each other, making these levels (including spin) fourfold degenerate; $\Lambda=0$ levels are twofold degenerate.

To describe the ground state, we assign to each cluster the value of δ for which the sum of single-particle energies is a minimum. The values of δ predicted for each cluster by this technique are shown in Fig. 2.

Now we correlate the features of the Nilsson model with the observed mass spectra. No explicit physical mechanism will be assumed *a priori* as the dominant process in producing the observed features; in fact, several independent effects may be contributing, including preferential formation of clusters with higher binding energy, variations in ionization efficiency as a function of N, and perhaps fragmentation. Instead, we only assume that, by whatever means, the variations in total electronic energy are primarily responsible for the sharp variations in the cluster mass spectra.

A convenient method for displaying variations in total energy as a function of N is described in Ref. 1. Applying this method to the Nilsson model, we compare the sum of single-particle energies of the N-atom cluster with clusters of $N-1$ and $N+1$ atoms by calculating the second difference:

$$\Delta_2(N)=\tfrac{1}{4}\{[E(N+1)-E(N)]-[E(N)-E(N-1)]\} \quad . \tag{3}$$

In this equation $E(N)$ is the sum of the single-particle energies for the N-atom cluster and ω_0 is approximated as constant for the three adjacent cluster sizes. The results are shown in Fig. 1(b) in dimensionless form for generality, but it should be kept in mind that the energy scale varies as $\omega_0(N)$, so that the peaks for the larger clusters appear exaggerated relative to those for the smaller clusters. The second difference of the sum of single-particle energies as a function of N is usually close to zero, unless an energy gap

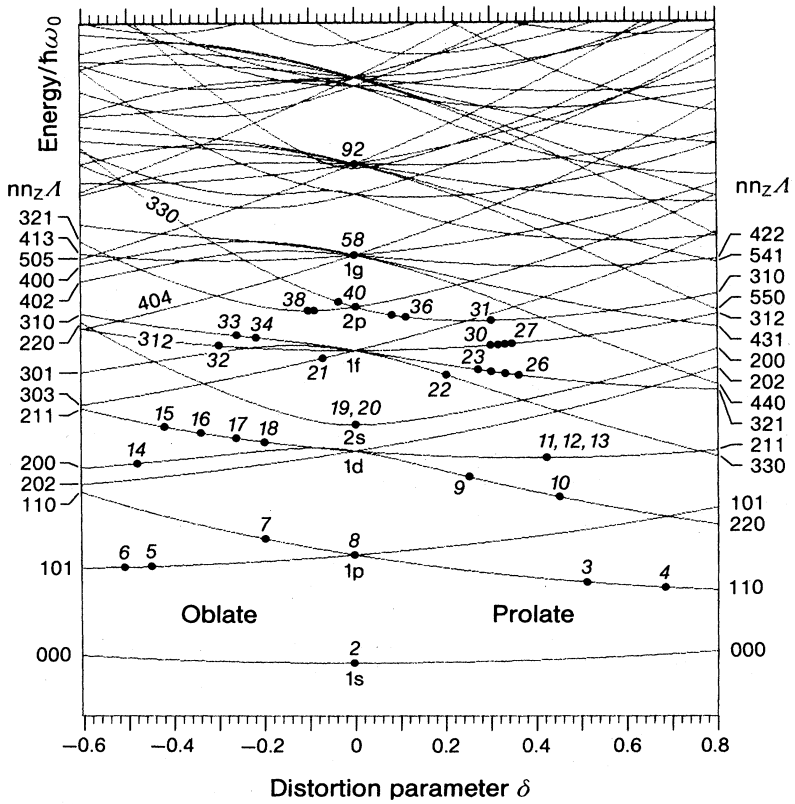

FIG. 2. Nilsson diagram of cluster energy levels as a function of the distortion parameter δ, for $U=0.04$. The energy scale is dimensionless in order to accommodate all cluster sizes, and the zero is suppressed; the $1s$-$1p$ energy difference at $\delta=0$ is exactly $\hbar\omega_0$. The points on the figure indicate the position of the highest occupied level for each cluster, at the value of δ corresponding to the assigned ground state.

separates the levels of the Nth and $(N+1)$th electrons; in this case $\Delta_2(N)$ becomes approximately the size of the energy gap.

The largest features in Fig. 1(b) reproduce the major spherical-shell closings, while the smaller features correspond to the filling of particular $|nn_z\Lambda\rangle$ subshells. These smaller peaks agree well with the structure observed in the mass spectra. In particular, the fourfold patterns in the $1f$ and $1g$ shells are correctly reproduced, the variation between $N=14$, 16, 18 is matched, and the twofold pattern in the $2p$ shell is understood as a case in which δ changes sign at midshell, so that a prolate subshell is filled at $N=36$ and an oblate subshell at $N=38$. The shell-closing peaks predicted by spherical theories at $N=18$, 34 remain in Fig. 1(b), but with magnitudes comparable to the adjacent ellipsoidal subshell peaks rather than to the other spherical-shell peaks. This is entirely consistent with the experimental data, and explains the absence of the major feature predicted by spherical jellium models at $N=34$.[4]

The only significant discrepancies between this model and the observed mass spectra occur in the range $N \leq 12$. This is to be expected, because the ellipsoidal approximation is less applicable to clusters with very few atoms. However, for the larger clusters the correlation between model and experiment is quite satisfactory throughout the range in which detailed features are observed in the mass spectra.

A comparison of Figs. 1 and 2 will show that the peaks appearing in $\Delta_2(N)$ typically correspond to energy gaps following shell or subshell closings, and the number N at which each closing occurs depends on the value of δ assigned to each cluster. In particular, it is clear from Fig. 2 that a change in the sign of δ usually implies a different set of subshell closings, which would result in different peak positions. Nearly all of the peak positions are properly matched, indicating that the ellipsoidal model correctly distinguishes the more likely geometry, prolate or oblate, in most cases.

The correlation between this simple model and the features observed in mass spectra suggests that even the finer details of the electronic enegy-level structure of free-electron metal clusters may be approximately described by considering only the energies of the valence electrons in a smooth axially symmetric potential, without specific information about the positions of the atomic cores. The cluster energy is minimized by relaxation of the cluster shape to conform more nearly to the shape of the available valence-electron wave functions. This assertion has been given detailed theoretical support for the smallest sodium clusters by Martins, Buttet, and Car.[11] They observe that when the atomic positions in a sodium cluster are allowed to relax, the eventual self-consistent wave functions for the valence electrons may be described as "s-like", "p-like", etc. Moreover, for the partially filled $1p$ shell clusters ($N=3$–7), they find cluster shapes which conform to the occupied p-like orbitals, differing from shapes generated by three-dimensional close-packing arguments. The variation from prolate to oblate geometry predicted by Nilsson theory for the $1p$ shell is consistent with the equilibrium geometries found in Ref. 11.

Several consequences of the ellipsoidal model are of interest. Measurements of the static electric polarizability of alkali-metal clusters[12] show that clusters with partially filled shells typically have a larger mean polarizability than nearby closed-shell clusters. The Nilsson Hamiltonian (with $U=0$ for simplicity) correctly describes this effect; when the polarizability is averaged over all orientations of the cluster, the result to second order in δ is[13]

$$\bar{\alpha}=\bar{\alpha}_{\delta=0}(1+\tfrac{4}{9}\delta^2)\ , \tag{4}$$

which shows small increases in $\bar{\alpha}$ for both prolate and oblate distortions. The ellipsoidal model may also offer a partial explanation for the discrepancies between spherical-shell calculations of photoionization potentials[3,4] and experimental results.[14] The large discontinuities in ionization potentials found at shell closings in the spherical theories are due to the size of the energy gap to the next available level. But in a nonspherical theory the clusters immediately following a closed shell are distorted, and this reduces the energy of the newly populated level, thus reducing the magnitude of the discontinuity in comparison with the values given by spherical theories.

The foregoing results suggest some possibilities for future experimental work. Plasma-resonance peaks, for example, will split into two peaks in the axially symmetric case, corresponding to the two scaling factors $\Omega_\perp$, Ω_z. This effect is analogous to the splitting of giant dipole-resonance peaks in nuclei,[15] and offers an experimental way to measure δ. Moreover, selection rules should be observed in the spherical and highly distorted limits, where the spherical and cylindrical representations are good descriptions of the actual eigenfunctions.

In conclusion, this model accounts for most of the smaller features of alkali-metal cluster mass spectra by relaxing the common spherical-shape constraint to allow clusters to assume energetically favorable ellipsoidal shapes. The experimental features which have previously been associated with spherical symmetry emerge naturally in the ellipsoidal model as special cases in which the ellipsoids reduce to spheres.

It is a pleasure to thank Professor Walter D. Knight, Walter de Heer, and Winston Saunders, each of whom has been generous with his time and advice throughout this project. I am grateful to Dr. W. Ekardt for criticizing the manuscript, and to Dr. Gary Schajer for assistance with numerical methods. This work was supported in part by the Materials Research Division of the U.S. National Science Foundation under Grant No. DMR 81-15540.

[1]W. D. Knight, K. Clemenger, W. A. de Heer, W. A. Saunders, M. Y. Chou, and M. L. Cohen, Phys. Rev. Lett. **52**, 2141 (1984).

[2]W. D. Knight, W. A. de Heer, K. Clemenger, and W. A. Saunders, Solid State Commun. **53**, 445 (1985).

[3]W. Ekardt, Phys. Rev. B **29**, 1558 (1984); D. E. Beck, Solid State Commun. **49**, 381 (1984); J. L. Martins, R. Car, and J. Buttet, Surf. Sci. **106**, 265 (1981). Very different structures occur in other kinds of clusters; cf. I. A. Harris, R. S. Kidwell, and J. A. Northby, Phys. Rev. Lett. **53**, 2390 (1984); L. A. Bloomfield, Bull. Am. Phys. Soc. **30**, 205 (1985).

[4]M. Y. Chou, A. Cleland, and M. L. Cohen, Solid State Commun. **52**, 645 (1984).

[5]S. G. Nilsson, K. Dan. Vidensk. Selsk. Mat. Fys. Medd. **29**, No. 16 (1955).

[6]C. Gustafson, I. L. Lamm, B. Nilsson, and S. G. Nilsson, Ark. Fys. **36**, 613 (1967).

[7]The **l** operator used in this paper is an ellipsoidal analog of the orbital angular momentum operator, defined in Appendix A of Ref. 5 as $\mathbf{l}_t$.

[8]A. Bohr and B. Mottelson, *Nuclear Structure: Vol. II, Nuclear Deformations* (Benjamin, Reading, MA, 1975), pp. 593–595.

[9]I am indebted to M. Y. Chou, A. Cleland, and M. L. Cohen for the use of their unpublished energy-level calculations.

[10]Ref. 8, pp. 231–233.

[11]J. L. Martins, J. Buttet, and R. Car, Phys. Rev. Lett. **53**, 655 (1984).

[12]W. D. Knight, K. Clemenger, W. A. de Heer, and W. A. Saunders, Phys. Rev. B **31**, 2539 (1985).

[13]K. Clemenger, Ph.D. dissertation, University of California, Berkeley, 1985 (unpublished).

[14]A. Herrmann, E. Schumacher, and L. Wöste, J. Chem. Phys. **68**, 2327 (1978); W. A. Saunders, K. Clemenger, W. A. de Heer, and W. D. Knight, Phys. Rev. B **32**, 1366 (1985), this issue.

[15]M. Danos, Nucl. Phys. **5**, 23 (1958); K. Okamoto, Phys. Rev. **110**, 143 (1958).